SLAC-PUB-14321

Single-Particle Dynamics in Electron Storage Rings with Extremely Low Emittance*

Yunhai Cai

SLAC National Accelerator Laboratory
Stanford University
Menlo Park, CA 94025

Abstract

Electron storage rings are widely used for high luminosity colliders, damping rings in high-energy linear colliders, and synchrotron light sources. They have become essential facilities to study high-energy physics and material and medical sciences. To further increase the luminosity of colliders or the brightness of synchrotron light sources, the beam emittance is being continually pushed downward, recently to the nanometer region. In the next decade, another order of reduction is expected. This requirement of ultra-low emittance presents many design challenges in beam dynamics, including better analysis of maps and improvement of dynamic apertures. To meet these challenges, we have refined transfer maps of common elements in storage rings and developed a new method to compute the resonance driving terms as they are built up along a beamline. The method is successfully applied to a design of PEP-X as a future light source with 100-pm emittance. As a result, we discovered many unexpected cancelations of the fourth-order resonance terms driven by sextupoles within an achromat.

An invited talk at the 8th International Conference in Charged Particle Optics, 12-16 July 2010, Singapore and submitted to Nuclear Instruments and Methods in Physics Research A

*Work supported by the Department of Energy under Contract No. DE-AC02-76SF00515.

1 Introduction

Computational tools have played an important role in the design of modern accelerators. During the 60's, K. Brown developed a first- and second-order matrix theory to design charged particle spectrometers. The matrix theory provided a powerful physics engine inside a code called TRANSPORT[1] for single-pass transport systems and later in MAD[2] for circular accelerators. An excellent feature of these matrix codes is that the linear matrices are the exact solutions of the linearized equations. For this reason, they are still widely used to design linear charged particle optics. However, for study of nonlinear dynamics, the second-order truncation might not be accurate enough and it also violates symplecticity, which is an intrinsic symmetry of Hamiltonian systems. In a storage ring, this violation itself might lead to artificial growth or damping when a particle is tracked in many thousands of turns.

In early the 80's, A. Dragt introduced and developed the Lie algebraic method[3] to the physics of charged particle optics. The Lie method laid a solid foundation for many modern codes. MARYLIE[4], the first design code based on the Lie algebra, has improved the accuracy by several orders but its transfer maps still violate sympecticity. To resolve this difficulty, E. Forest utilized the technique of high-order canonical integrators[5] and developed a tracking code called DESPOT[6]. Later these integrators were implemented in many other codes such as LEGO[7] in the C++ language. In addition to the preservation of symplecticity, these codes, equipped with the differential algebra[8], can be used efficiently and accurately to extract a Taylor map in an arbitrary order. However, in practice, since these integrators are constructed by a combination of drifts and kicks, these tracking codes cannot provide the exact linear transfer matrices as those in the design codes such as MAD. For this reason, these tracking codes were never seriously used to design the linear optics of charged particles.

Can we improve these tracking codes so that they can be also used as design codes? How can we develop a code that retains all advantages of the existing codes? These are the questions that will be answered in the first part of this paper. In section 2, we will introduce a general Hamiltonian of magnets in circular accelerators. Then we will solve its Hamiltonian equations for several common elements in section 3. For a nonlinear system, we will introduce the Lie algebraic method and then lead to a symplectic integrator to approximate the system in section 4.

In the second part of the paper, we will develop a new method to calculate the resonance driving terms of an arbitrary order along a beamline in section 5. Then we will apply it to study the resonance terms driven by sextupole magnets in a lattice that consists of many achromats. Many coincidental cancelations will be uncovered and their impacts on the dynamic aperture will be investigated in section 7. Finally we will discuss other possible applications.

2 Hamiltonian

In a modern storage ring, there are three types of basic magnets. They play a unique role and are absolutely essential. First, dipoles bend charged particles and define the geometry. Second, quadupoles provide focus to the particles so that they continually oscillate around a design orbit. Finally, sextupoles compensate chromatic effects in the quadrupole focusing system. For these types of magnetic elements, we can easily introduce a simple Hamiltonian to describe the dynamics of a charged particle in the storage ring.

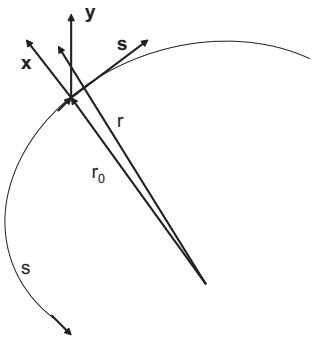

Figure 1: *The planar curved coordinate system.*

Consider a sector bending magnet with magnetic field B_0 in a curved coordinate system with radius ρ as illustrated in Fig 1. It is well known that if one uses the design path length s as an independent variable, its Hamiltonian can be written as[9]

$$H = -(1+\frac{x}{\rho})\sqrt{(1+\delta)^2 - p_x^2 - p_y^2} + \frac{x}{\rho} + \frac{x^2}{2\rho^2} - \frac{A_s(x,y)}{B_0\rho}, \tag{2.1}$$

where $\delta = (P - P_0)/P_0$ is the relative momentum deviation from $P_0 = eB_0\rho$ the momentum of an ideal particle with charge e, p_x and p_y are canonical momenta corresponding to the coordinates x and y respectively, and $A_s(x, y)$ is the longitudinal component of vector potential. In this paper, we choose the canonical coordinates $z = (x, p_x, y, p_y, \delta, \ell)$. Here $\ell = c\tau$, c is speed of light, and τ the time of flight. For simplicity, we have assumed that the charged particle has very high energy and is fully ultra-relativistic.

We also assumed that the bending radius has perfectly matched ρ in the curved coordinate system and deviations of magnetic errors are included in $A_s(x, y)$ which can be described with the multipole expansion

$$A_s = -Re[\sum_{n=1} \frac{1}{n}(b_n + ia_n)(x + iy)^n], \tag{2.2}$$

where b_n and a_n are the normal and skew components of multipoles respectively. In our convention, b_3 is for a normal sextupole. The magnetic field can be computed from the vector potential using $\vec{B} = \nabla \times \vec{A}$. The result is

$$B_y + iB_x = \sum_{n=1}(b_n + ia_n)(x + iy)^{n-1}. \tag{2.3}$$

When a machine is large ($x << \rho$) and the angles are small $p_x << 1, p_y << 1$, we can further simplify the Hamiltonian in Eq. 2.1 by expanding the square root and keeping only the quadratic terms in p_x and p_y. The Hamiltonian becomes[6]

$$H = \frac{p_x^2 + p_y^2}{2(1 + \delta)} - \frac{x\delta}{\rho} + \frac{x^2}{2\rho^2} - \frac{A_s(x, y)}{B_0\rho}. \tag{2.4}$$

We have dropped the term $-(1 + \rho)$ by redefining ℓ as the path length relative to the ideal one. In Eq. 2.4, $-x\delta/\rho$ describes the bending dispersion and $x^2/(2\rho^2)$ the weak focusing due to the curvature. Given a Hamiltonian such as Eq. 2.4, the motion of a charged particle can be described precisely by the solution of the Hamiltonian equation

$$\frac{dq_i}{ds} = \frac{\partial H}{\partial p_i}, \frac{dp_i}{ds} = -\frac{\partial H}{\partial q_i}. \tag{2.5}$$

Here we note that $q_{1,2,3} = x, y, \delta$ as the coordinates and $p_{1,2,3} = p_x, p_y, \ell$ their corresponding canonical momenta.

3 Solvable Hamiltonian systems

By selecting a different combination of parameters, ρ, a_n, and b_n in Eq. 2.4, we will apply the Hamiltonian for a drift space, dipole, quadrupole, or sextupole magnet.

3.1 Drift space

In a realistic storage ring, drift spaces are necessary due to the gaps and empty space between the accelerator components. To obtain the Hamiltonian of a drift space, we simply set $A_s = 0$ and take the limit of ρ to infinity in Eq. 2.4

$$H_{drift} = \frac{p_x^2 + p_y^2}{2(1+\delta)}. \tag{3.1}$$

Since H_{drift} does not depend on $x, y,\ \ell$, their conjugates p_x, p_y, δ are the constants of motion. Solving the Hamiltonian equations for the other three variables, we have

$$\begin{aligned} x(\Delta s) &= x + \frac{\Delta s p_x}{(1+\delta)}, \\ y(\Delta s) &= y + \frac{\Delta s p_y}{(1+\delta)}, \\ \ell(\Delta s) &= \ell + \frac{\Delta s (p_x^2 + p_y^2)}{2(1+\delta)^2}, \end{aligned} \tag{3.2}$$

where Δs is the distance from the entry of the drift. For simplicity, we take $x, p_x, y, p_y, \delta, \ell$ as their values at the entry of the drift space.

3.2 Sector bend

As we mentioned earlier, the dipole magnets are the most important element in a storage ring because they bend the charge particles and therefore define the layout of the ring. The simplest dipole is a sector bend which is defined as a dipole magnet of uniform field with both edges perpendicular to the bending circle. In the curved coordinate shown in Fig. 1, we have

$$H_{sbend} = \frac{p_x^2 + p_y^2}{2(1+\delta)} - \frac{x}{\rho}\delta + \frac{x^2}{2\rho^2}, \tag{3.3}$$

which is obtained by setting $A_s = 0$ in Eq. 2.4. It is clear that δ and p_y are two constants of motion. For the rest, by solving its Hamiltonian equations, we have

$$\begin{aligned}
x(\Delta s) &= x\cos(k\Delta s) + \frac{p_x}{k(1+\delta)}\sin(k\Delta s) + \rho\delta[1-\cos(k\Delta s)], \\
p_x(\Delta s) &= p_x\cos(k\Delta s) - xk(1+\delta)\sin(k\Delta s) + k(1+\delta)\rho\delta\sin(k\Delta s), \\
y(\Delta s) &= y + \frac{\Delta s p_y}{(1+\delta)}, \\
\ell(\Delta s) &= \ell + \Delta s\delta + (\frac{x}{\rho}-\delta)\frac{\sin(k\Delta s)}{k} + p_x\rho[1-\cos(k\Delta s)] \\
&\quad + \frac{1}{2(1+\delta)^2}\{\Delta s p_y^2 + \frac{s}{2}[p_x^2 + (1+\delta)(\frac{x}{\rho}-\delta)^2] \\
&\quad - p_x\rho(1+\delta)(\frac{x}{\rho}-\delta)\sin^2(k\Delta s) \\
&\quad + [p_x^2 - (1+\delta)(\frac{x}{\rho}-\delta)^2]\frac{\sin(2k\Delta s)}{4k}\}, \qquad (3.4)
\end{aligned}$$

where $k = 1/(\rho\sqrt{1+\delta})$. In a sector bend, the motion in the vertical plane is the same as in drift space. But in the horizontal plane, it has a harmonic oscillation due the weak focusing and dispersion driven by a radius $\delta\rho$ with a variation of energy δ.

3.3 Quadrupole

As we have shown previously, the particle in a dipole drifts in the vertical plane. In general, a charged particle orbiting in a uniform magnetic dipole field is not confined if there is a small perturbation in its vertical velocity. Quadrupole magnets are necessary to provide focusing and stabilize the motion. More often, quadrupoles are used to reduce the beam size at an interaction point in colliders or to minimize the equilibrium emittance in electron storage rings. The quadrupole Hamiltonian can be derived by setting $a_n = b_n = 0$ except b_2 and take the limit of ρ to infinity in Eq. 2.4 to give

$$H_{quad} = \frac{p_x^2 + p_y^2}{2(1+\delta)} + \frac{K_1}{2}(x^2 - y^2), \qquad (3.5)$$

where $K_1 = b_2/(B_0\rho)$ and $(B_0\rho)$ is the magnetic rigidity determined by the design energy $E_0 = cP_0$ of the storage ring. Again, δ is a constant of the

motion. For a focusing quadrupole, $K_1 > 0$, the rest can be obtained by solving the Hamiltonian equations

$$\begin{aligned}
x(\Delta s) &= x\cos(k\Delta s) + \frac{p_x}{k(1+\delta)}\sin(k\Delta s), \\
p_x(\Delta s) &= p_x\cos(k\Delta s) - k(1+\delta)x\sin(k\Delta s), \\
y(\Delta s) &= y\cosh(k\Delta s) + \frac{p_y}{k(1+\delta)}\sinh(k\Delta s), \\
p_y(\Delta s) &= p_y\cosh(k\Delta s) + k(1+\delta)y\sinh(k\Delta s), \\
\ell(\Delta s) &= \ell + \frac{1}{2(1+\delta)^2}\{\frac{\Delta s}{2}[p_x^2 + (1+\delta)^2k^2x^2] \\
&\quad + \frac{1}{4k}[p_x^2 - (1+\delta)^2k^2x^2]\sin(2k\Delta s) \\
&\quad + \frac{1}{2}(1+\delta)xp_x[\cos(2k\Delta s) - 1] \\
&\quad + \frac{\Delta s}{2}[p_y^2 - (1+\delta)^2k^2y^2] \\
&\quad + \frac{1}{4k}[p_y^2 + (1+\delta)^2k^2y^2]\sinh(2k\Delta s) \\
&\quad + \frac{1}{2}(1+\delta)yp_y[\cosh(2k\Delta s) - 1]\}, \qquad (3.6)
\end{aligned}$$

where $k = \sqrt{|K_1|/(1+\delta)}$. For the solution of a defocusing quadrupole, $K_1 < 0$, one simply needs to swap x and y, including in the subscripts in Eq. 3.6.

As one can see, the transfer maps discussed in this section have non trivial nonlinear components. However, the symplecticity is preserved because they are the exact solutions of the Hamiltonian equation. In fact, this can be directly verified using their Jacobians.

It is worth noting that the linear parts of these transfer maps are the same as those in a design code such as MAD, with a proper swap of the fifth and sixth canonical coordinates. Furthermore, there are more solvable systems such as a combined function magnet of a dipole and a quadrupole. Due to space limitations, they will not be reported in this paper.

4 Lie algebraic method

The Lie algebraic method for charged particle optics was introduced and developed by A. Dragt[3]. It emphasizes exponential Lie operators that are similar to those in quantum field theory.

4.1 Exponential Lie operator

When a Hamiltonian such as the one in Eq. 2.4 does not have any explicit dependence on the independent variable s, we can show[10]

$$f(q_1(\Delta s), p_1(\Delta s), ...) = e^{-\Delta s:H:} f(q_1, p_1, ...), \tag{4.1}$$

where f is a function of the coordinates q_i and their canonical conjugates p_i and the Lie operator $e^{-\Delta s:H:}$ is defined as the Taylor expansion

$$e^{-\Delta s:H:} f = f + [-\Delta s H, f] + \frac{1}{2!}[-\Delta s H, [-\Delta s H, f]] + ..., \tag{4.2}$$

where $[h, f]$ is defined by the Poisson bracket

$$[h, f] = \sum_i (\frac{\partial h}{\partial q_i}\frac{\partial f}{\partial p_i} - \frac{\partial h}{\partial p_i}\frac{\partial f}{\partial q_i}). \tag{4.3}$$

As one can easily see from Eq. 4.1 if one chooses f as an individual coordinate q_i or its conjugate p_i, the Lie operation $e^{-\Delta s:H:}$ also represents the transfer map of $z = (x, p_x, y, p_y, \delta, \ell)$ from the entry to the exit of an element. In fact, the transfer maps found in the previous section can also be derived by directly applying their corresponding Lie operators and computing the Poisson brackets. However, as one will find out quickly, it can be a tedious process to derive the transfer map this way. Nevertheless, the Lie operator is a very useful presentation of the transfer map, as one will see in the next section.

4.2 Sextupole

As one can see in Eq 3.6, the transfer map of a quadrupole is a function of the energy deviation δ. As a result, the sextupole magnets placed in dispersive regions are necessary to compensate the chromatic effects from quadrupoles. For a sextupole magnet, the Hamiltonian can be derived by

setting $a_n = b_n = 0$ except b_3 and take the limit of ρ to infinity in Eq. 2.4. The result is

$$H_{sext} = \frac{p_x^2 + p_y^2}{2(1+\delta)} + \frac{K_2}{3!}(x^3 - 3xy^2), \tag{4.4}$$

where $K_2 = 2b_3/(B_0\rho)$. Due to the nonlinear potential

$$H_s(x,y) = \frac{K_2}{3!}(x^3 - 3xy^2), \tag{4.5}$$

the Hamiltonian equations of the sextupole cannot be solved exactly. But, as discussed earlier, we can still write its transfer map formally as

$$\mathcal{M}_{sext} = e^{-\Delta s:H_{sext}:}, \tag{4.6}$$

where Δs is the length of the sextupole. This Lie presentation allows us to make an approximation

$$e^{-\Delta s:H_{sext}:} = e^{-\frac{\Delta s}{2}:H_{drift}:} e^{-\Delta s:H_s:} e^{-\frac{\Delta s}{2}:H_{drift}:} + O(\Delta s^3), \tag{4.7}$$

which can be proven by applying the Cambell-Baker-Hausdorf (CBH) theorem

$$e^{:A:} e^{:B:} = e^{:C:}, \tag{4.8}$$

where

$$C = A + B + \frac{1}{2}[A,B] + ... \tag{4.9}$$

As shown by Eq. 4.7, the map of a sextupole can be approximated by inserting a lumped kick

$$\begin{aligned} p_x(0^+) &= p_x - \Delta s \frac{\partial H_s}{\partial x}, \\ p_y(0^+) &= p_y - \Delta s \frac{\partial H_s}{\partial y}, \end{aligned} \tag{4.10}$$

in the middle of the drift. It is obvious that this approximation preserves the symplecticity. Moreover, its residual error is in third order of Δs so it is often called a second-order symplectic integrator. To further reduce the error, one can first divide the magnet into many identical segments and then use the integrator for each segment.

It is worth noting that the method of symplectic integrator can be applied to many systems. For example, to treat a combined function magnet of a quadrupole and a sextupole, one simply uses H_{quad} instead of H_{dirft} in Eq. 4.7.

5 Analysis of maps

As we have shown in the previous sections, a transfer map of an element in an accelerator can be obtained simply by solving its Hamiltonian equations. Or if the Hamiltonian system is not solvable, we can use a symplectic integrator to approximate the system. For a beamline constructed with a sequence of elements, its transfer map is the nested map concatenated sequentially from the maps of the elements. In principle, one can apply a sequence of substitutions to obtain the explicit map. In fact, it can be shown that this procedure also preserves symplecticity. In practice, no one uses it because there are too many elements in a modern storage ring. Once again, some approximations are necessary.

5.1 Truncated Taylor map

An idea pioneered by M. Berz[8] is to use a truncated power series (TPS)

$$f(q_1, p_1, ...) = \sum_{k_1,...,k_6=0}^{k_1+...+k_6 \le o} D^f_{k_1,...,k_6} q_1^{k_1} p_1^{k_2} q_2^{k_3} p_2^{k_4} q_3^{k_5} p_3^{k_6}, \tag{5.1}$$

to approximate the transfer map. For simplicity, we assume that the order of truncation o is fixed. There are several advantages of this approach. First, the TPS are essentially polynomials of a few variables so one can define simple and natural rules, called differential algebra[8], to manipulate them. Second, if ones use the TPS to represent q_i and p_i, a truncated Taylor map of a beamline can be extracted simply by starting with an identity map and then tracking it through as if it is a ray of the phase space. In a modern computer language such as C^{++}, this property, called polymorphism, allows us to write a much simpler code to handle both ray tracing and map extracting. A good implementation of the polymorphism also provides a consistency between the ray tracing and the analysis of the maps. Third, a Taylor map is also a natural choice from a perturbation point of view since q_i and p_i are small and often oscillate around zero in storage rings. In particular, its linear part is identical to the transfer matrix in the design codes TRANSPORT and MAD and in the theory of Courant-Snyder[11]. Finally and most importantly, the differential algebra is a much more accurate method for computing high derivatives than using numerical differences.

As usual, a Taylor map has its short comings. First, the series may not be convergent as q_i or p_i become large. Second, some physics might be left out

due to the truncation. Finally, the truncation itself violates the symplecticy. This might lead to artificial growth or damping if it is used in ray tracing[12].

5.2 Lie factorization

A method to restore the symplecticity of a Taylor map $\mathcal{M}$ is to use the Dragt-Finn procedure[13]

$$\mathcal{M} = \mathcal{M}^1 e^{:f_3(z):} e^{:f_4(z):} ..., \tag{5.2}$$

to represent it as a product of exponential Lie operators with a homogeneous polynomial $f_n(z)$ of increasing order n. Here we note $\mathcal{M}^1$ as its linear part. For a Taylor map truncated at order o, the procedure of the factorization only ensures the validity of the equal sign up to the order o. The other terms beyond the order of the truncation on the right hand side of Eq. 5.2 are necessary to recover the symplecticity.

5.3 Single Lie factor

Applying the CBH theorem in Eqs. 4.8 and 4.9 to the Dragt-Finn factorization in Eq. 5.2 , we can combine the product of the exponential Lie operators into a single Lie factor

$$\mathcal{M} \;=\; \mathcal{M}^1 e^{:f_3(z)+f_4(z)+\ldots:}. \tag{5.3}$$

Here we have used the fact that the Poisson bracket of f_3 and f_4 gives a fifth-order polynomial. As a result, f_3 and f_4 in the Dragt-Finn factorization are numerically identical to those in the single Lie factor.

When $\mathcal{M}$ is the one-turn map of a storage ring, the single Lie factor is often used to compute the driving terms of nonlinear resonances. Here we want to focus on an arbitrary segment of the storage ring and try to find an extension of such an analysis to see how the driving terms are built up along the entire ring.

5.4 Normalized coordinates

Consider $\mathcal{M}$ as a transfer map for position 1 to 2 in a storage ring. It is well known that its linear part can be written as

$$\mathcal{M}^1 = \mathcal{A}_1^{-1} \mathcal{R}_{12} \mathcal{A}_2, \tag{5.4}$$

where $\mathcal{R}_{12}$ is a linear map of rotation, $\mathcal{A}_1^{-1}$ is a linear transformation to the normalized coordinate at the position 1, and $\mathcal{A}_2$ is a transformation back to the original phase space at the position 2. In general, $\mathcal{A}(s)$ can be constructed easily using the eigen vectors of the one-turn matrix at position s and $\mathcal{R}_{12}$ by three phase advances in the eigen planes.

For an ideal lattice without any linear coupling, we have a block diagonal form of $\mathcal{A}$. Its nonzero block of a 2×2 matrix has the form of

$$A_{2\times 2} = \begin{pmatrix} \sqrt{\beta} & 0 \\ -\frac{\alpha}{\sqrt{\beta}} & \frac{1}{\sqrt{\beta}} \end{pmatrix}, \tag{5.5}$$

where β and α are the Courant-Synder parameters.

Substituting Eq. 5.4 into Eq. 5.3, we obtain

$$\mathcal{M} = \mathcal{A}_1^{-1}\mathcal{R}_{12}e^{:f_3(\mathcal{A}_2 z)+f_4(\mathcal{A}_2 z)+\ldots:}\mathcal{A}_2. \tag{5.6}$$

Here we have used a general property[10] of a similar transformation for an exponential Lie operator

$$\mathcal{B}e^{:f(z):}\mathcal{B}^{-1} = e^{:f(\mathcal{B}z):}, \tag{5.7}$$

where $\mathcal{B}$ is an arbitrary exponential Lie operator.

5.5 Resonance bases

To compute the driving terms of resonances, it is more convenient to make another complex but symplectic transformation[14] to diagonalize $\mathcal{R}_{12}$

$$\mathcal{R}_{12} = \mathcal{K}\Lambda_{12}\mathcal{K}^{-1}, \tag{5.8}$$

where $\mathcal{K}$ is the block diagonal and its nonzero block of a 2×2 matrix has the form of

$$K_{2\times 2} = \frac{1}{\sqrt{2}} \begin{pmatrix} 1 & -i \\ -i & 1 \end{pmatrix}. \tag{5.9}$$

Substituting Eq. 5.8 into Eq. 5.6 and using the similarity transformation in Eq. 5.7, we have

$$\mathcal{M} = \mathcal{A}_1^{-1}\mathcal{K}\Lambda_{12}e^{:f_3(\mathcal{A}_2\mathcal{K}^{-1} z)+f_4(\mathcal{A}_2\mathcal{K}^{-1} z)+\ldots:}\mathcal{K}^{-1}\mathcal{A}_2. \tag{5.10}$$

The coefficients of the Lie operator in the exponential defines all driving terms of resonances between points 1 and 2. For example, the term with indexes of $(3,0,0,0,0,0)$ or $(0,3,0,0,0,0)$ leads to the $3\nu_x$ resonance.

As one can see from Eq. 5.10, it is rather simple to calculate the third and fourth order driving terms along the entire ring. Here is a practical procedure:

- search the closed orbit at the beginning;
- initialize an identity map with respect to the closed orbit;
- propagate the transfer map to the next element;
- perform the Dragt-Finn factorization to find f_3 and f_4;
- apply transformation $\mathcal{A}^\dagger$ and then $\mathcal{K}^{-1}$ to f_3 and f_4;
- write out the result and loop back to the third item until the end.

This procedure, along with the transfer maps of the solvable Hamiltonian system discussed in the previous sections, has been recently implemented in LEGO[7]. In the next section, we will apply this to analyze the nonlinearity in storage rings.

6 Application

PEP-X[15] is a possible future synchrotron light source residing in the existing PEP tunnel at SLAC. After several years of study, a baseline design[16] was recently completed. The design promises photon beams that achieve a brightness of 10^{22} (ph/s/mm^2/mrad^2/0.1% BW) at 10 keV in a conventional planar undulator. In this paper, we will use a simplified lattice, entirely made with theoretical minimum emittance (TME) cells in the arcs, to study the dynamics of a charged particle.

The TME cell phase advances are chosen to be, $\mu_x = 135^0$ and $\mu_y = 45^0$, so that all third-order geometrical aberrations generated by sextupoles are canceled within an achromat[17], which consists of eight cells that make a identity transformation in both the horizontal and vertical planes. Higher phase advance in the horizontal plane is necessary to make lower emittance.

[†]propagated as a linear map as well

The choice of phase advances also helps to reduce the chromatic betatron beating. The optics of one TME cell is shown in Fig. 2. The polarity of quadrupoles is selected to efficiently reduce the emittance without too much focusing. Bending magnets are made as long as reasonably possible in order to maximize the momentum compaction factor for a longer bunch length and to minimize the emittance. As one can see in Fig. 2, there are two families of sextupoles placed symmetrically for chromaticity correction.

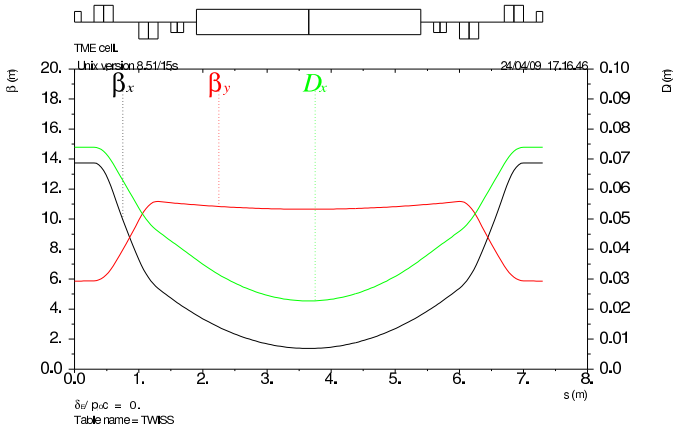

Figure 2: *Optics functions in one TME cell.*

Each arc consists of four achromats and ends with a dispersion suppressor. The ring has six identical arcs interconnected with six straight sections equipped with simple FODO cells without any dispersions. The main parameters of the storage ring are tabulated in Table 1.

In this study, we set the strengths of sextupoles in the two families to zero out the linear chromaticity in the ring and then carried out the procedure outlined in the end of the previous section. For the third-order resonances, the contribution of sextupoles to all driving terms along the PEP-X storage ring are plotted in Fig. 3. As one can see from the figure, they are all canceled out within each achromat (made with eight cells), as predicted by the theorem[17]. This servers as a good benchmark of the code versus the analytical perturbation theory.

For the fourth-order resonances, we find similar cancelations as shown in Fig. 4 except for one resonance: $2\nu_x + 2\nu_y = 258$. These accidental cancelations can not be explained by the first-order perturbation theory[17]. However, they are confirmed by applying the CBH theorem and computing

Table 1: Main parameters of a design of PEP-X as an ultra-low emittance storage ring.

Parameter	Description	Value
E_0 [GeV]	beam energy	4.5
C [m]	circumference	2199.32
ϵ_x [pm-rad]	horizontal emittance	94.6
τ_t [ms]	damping time	202
ν_x,ν_y,ν_s	tunes	89.66, 39.57, 0.003
ξ_x, ξ_y	natural chromaticity	-149.62, -64.12
α_c	momentum compaction	7.58×10^{-5}
σ_z [mm]	bunch length	3.00
σ_e/E	energy spread	3.6×10^{-4}
U_0 [MeV]	energy loss per turn	0.33
V_{RF} [MV]	RF voltage	1.16

the Poisson brackets of H_s (Eq. 4.5) for all pairs of sextupoles inside the achromat. Due to space limitations, the analytic calculation based on the Lie algebraic method will be reported elsewhere.

In order to cancel the only remaining driving term of the resonance $2\nu_x + 2\nu_y$ in the entire ring, we adjusted the phase advances in three straight sections so that the term was eliminated in a pair of arcs. Finally, we developed a lattice without any geometrical resonance excitations up to fourth order. However, it is worth to noting that there are still three terms of geometric aberrations in f_4. They do not drive any resonances but generate the changes of betatron tunes.

To investigate if the elimination of the resonance terms has any positive effect on the dynamic aperture, we scanned the betatron tunes within one unit in the horizontal and vertical planes. At every point in the tune plane, we tracked the on-momentum particles up to a thousand turns and determine the dynamic apertures in x, y, and diagonal directions. The scanning result of the minimum aperture in the three directions is shown in Fig. 5. Some residual effects of the resonance $2\nu_x + 2\nu_y = 258$ are clearly seen in the figure. This might be a deficiency of the long range cancelation between the two arcs in which the driving term has been built up significantly. There

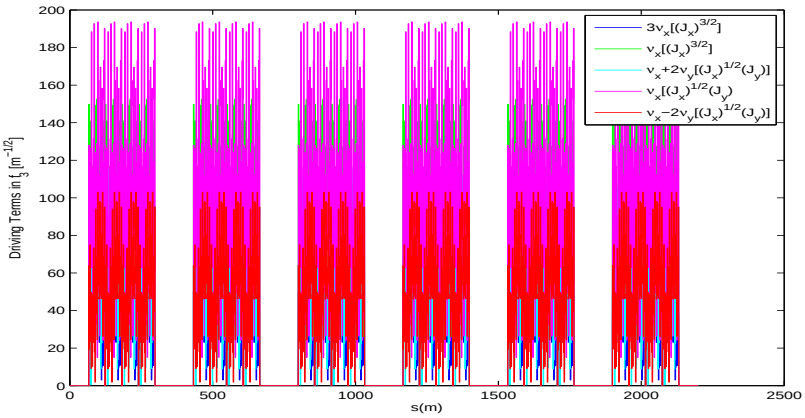

Figure 3: *All third-order resonances driven by sextupole magnets.*

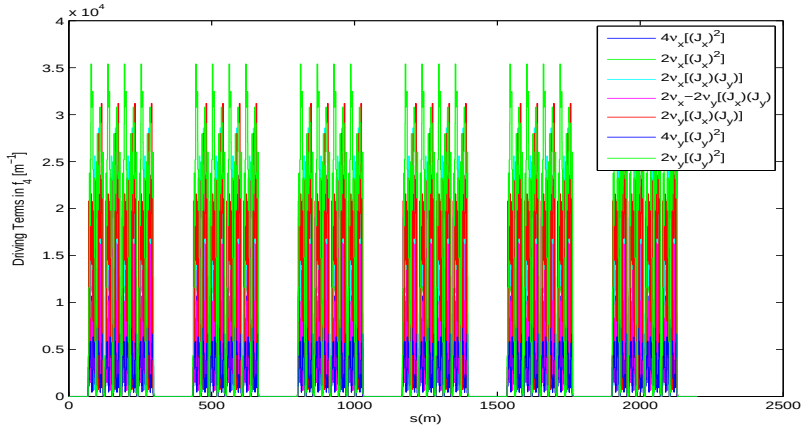

Figure 4: *Fourth-order resonances driven by sextupole magnets.*

were no identifiable degradations due to the other third and fourth order resonances. Clearly, this achromatic lattice has good dynamic apertures in a large area in the tune plane.

In order to see the degradation of dynamic aperture when the driving terms are not minimized, we increased in the phase advance by 5^0 in both planes in the cell, rematched the lattice, and corrected the linear chromaticity. As a result of this change, we violated the conditions of being an achromat. We scanned the dynamic aperture for the detuned lattice. The result of this is shown in Fig. 6 for a comparison to Fig. 5. One sees that a large area of tune space is wiped out by the strong horizontal resonances. A similar result was found for a lattice with 5^0 decrease in the phase advances.

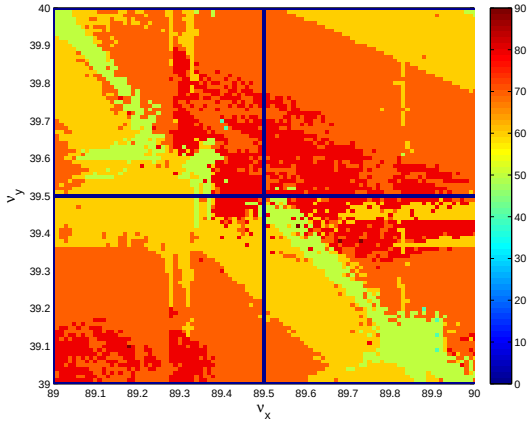

Figure 5: *Dynamic aperture (in unit of σ of a beam with emittance $\epsilon_x = \epsilon_y = 100$ pm-rad) as a function betatron tunes for the achromatic lattice of PEP-X.*

7 Discussion

Our results clearly show that the lattice built with achromats has much more operating space in the tune plane due to many cancelations of the driving terms of low-order resonances. We have found that the additional cancelations of the 4th-order driving terms in the achromat are very general. They do not depend on a particular type of cell, not on the number of sextupole families , not on the positions of sextupoles, and not even on their strengths and lengths. All these freedoms can be used to further optimize tune shifts, chromaticity, and dynamic aperture.

Obviously, the methods developed in this paper can also be applied to proton storage rings, where the symplecticity is much more important. However, in proton machines, sextupoles might not be the only dominate sources of nonlinearity as in electron rings (especially at a limit of ultra-low emittance). For example, the multipole errors in the dipole magnets may be necessary for the study of the resonance driving terms and the dynamic aperture. Even for this complicated situation, our method of calculating driving terms is still applicable. Moreover, our method of analysis can also be used in a single-pass system when an initial map is given.

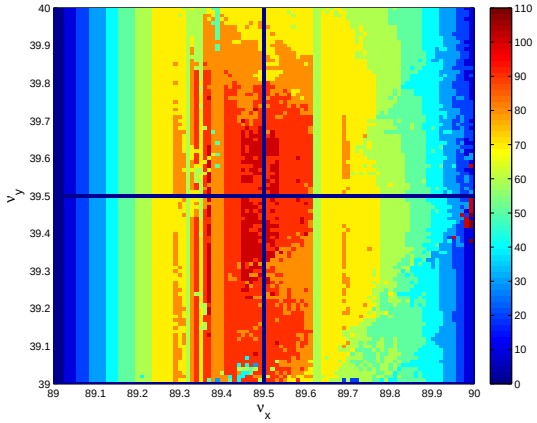

Figure 6: *Dynamic aperture (in unit of σ of a beam with emittance $\epsilon_x = \epsilon_y =$ 100 pm-rad) as a function betatron tunes for a lattice with an increase of 5^0 in phase advances per cell.*

Acknowledgments

I would like to thank my colleagues who worked on the design of PEP-X for many helpful and stimulating discussions. This work was supported by the Department of Energy under Contract Number: DE-AC02-76SF00515.

References

[1] K.L. Brown, "A First- and Second-Order Matrix Theory for the Design of Beam Transport Systems and Charged Particle Spectrometers," SLAC Rep. No 75; Adv. Particle Phys. **1** 71-134 (1967).

[2] H. Grote and F. C. Iselin, "The MAD Program (Methodical Accelerator Design) Version 8.15," CERN/SL/90-13 (AP), (1990).

[3] A.J. Dragt, "Lie algebraic theory of geometrical optics and optical aberrations," J. Opt. Soc. Am., **72**, 372 (1982). A. Dragt *et al.* "Lie algebraic treatment of linear nonlinear beam dynamics", Ann. Rev. Nucl. Part. Sci., **38**, 455 (1988).

[4] A.J. Dragt, L.M. Healy, F. Neri, R.D. Ryne, D.R. Douglas, and E. Forest, "MARYLIE 3.0 - A Program for Nonlinear Analysis of Accelrator and Beamline Lattices," IEEE Trans. Nucl. Sci. **NS-32**, No. 5, 2311 (1985).

[5] R. D. Ruth, "A Canonical Integration Technique," IEEE Trans. Nucl. Sci. **NS-30**, No.4, 2669 (1983).

[6] E. Forest, "Canonical Integrators as Tracking Codes," SSC-138, (1987).

[7] Y. Cai, M. Donald, J. Irwin, Y. Yan, "LEGO: A Modular Accelerator Design Code," SLAC-PUB-7642, August (1997).

[8] M. Berz, "Differential Algebra Description of Beam Dynamics to Very High Order," Part. Accel. **24**, 109 (1989).

[9] R.D. Ruth, "Single Particle Dynamics in Circular Accelerator," AIP Conference Proceedings No. 153, Vol.1 p166, M. Month and M. Dienes editors (1985).

[10] J. Irwin, "The Application of Lie Algebra Techniques to Beam Transport Design," SLAC-PUB-5315, Nucl. Instrum. Methods, **A298**, 460 (1990).

[11] E.D. Courant and H.S. Snyder, "Theory of the Alternating-Gradient Synchrotron," Annals of Physics: **3**, 1-48 (1958).

[12] R.L. Warnock, Y. Cai, and J.A. Ellison, "Construction of Large-Period Symplectic Maps by Interpilative Method," SLAC-PUB-13867, December (2009).

[13] A.J. Dragt and J.M. Finn, "Lie Series and invariant functions for analytic symplectic maps," J. Math. Phys. **17**, 2215 (1976).

[14] E. Forest, M. Berz, and J. Irwin, "Normal Form Methods for Complicated Periodic Systems: A Complete Solution Using Differential Algebra and Lie Operators," Part. Accel. **24** 91 (1989).

[15] R.O. Hettel *et al.*, "Ideas of a Future PEP Light Source," EPAC08-WEPC023 (2008).

[16] Y. Cai *et al.*, "A Baseline Design for PEP-X: An Ultra-Low Emittance Storage Ring," IPAC'10, (2010).

[17] K.L. Brown and R.V. Servranckx, "Optics Modules for Circular Accelerator Design," Nucl. Instrum. Methods, **A258**, 480 (1987).